Radiocarbon in dissolved organic carbon of the Atlantic Ocean

Druffel, Ellen R M ; Griffin, Sheila ; Coppola, Alysha I ; Walker, Brett D

Abstract: Marine dissolved organic carbon (DOC) is produced in the surface ocean though its radiocarbon (^{1}C) age in the deep ocean is thousands of years old. Here we show that >10% of the DOC in the deep North Atlantic is of post-bomb origin and that the ^{1}C age of pre-bomb DOC is >4900 ^{1}C yr, 900 ^{1}C yr older than previous estimates. We report ^{1}C ages of DOC in the deep South Atlantic that are intermediate between values in the North Atlantic and the Southern Ocean. Finally, we conclude that DOC ^{1}C ages are older and a portion of deep DOC is more dynamic than previously reported.

DOI: https://doi.org/10.1002/2016GL068746

Geophysical Research Letters

Supporting Information for

Dissolved organic carbon in the Atlantic Ocean using bomb ^{14}C

E. R. M. Druffel, S. Griffin, A. I. Coppola and B. D. Walker

Department of Earth System Science, U. C. Irvine, Irvine, CA 92697-3100

Contents of this file

Introduction

The data contained in this file describe the sampling information for water samples reported in the paper and those used for comparison. Details of the $\Delta^{14}C$ and ^{13}C analyses are included in the Methods section of the paper. The DOC concentrations, and DOC $\Delta^{14}C$ and ^{13}C values are listed in Table S2. Error estimates are included in the Methods section of the paper.

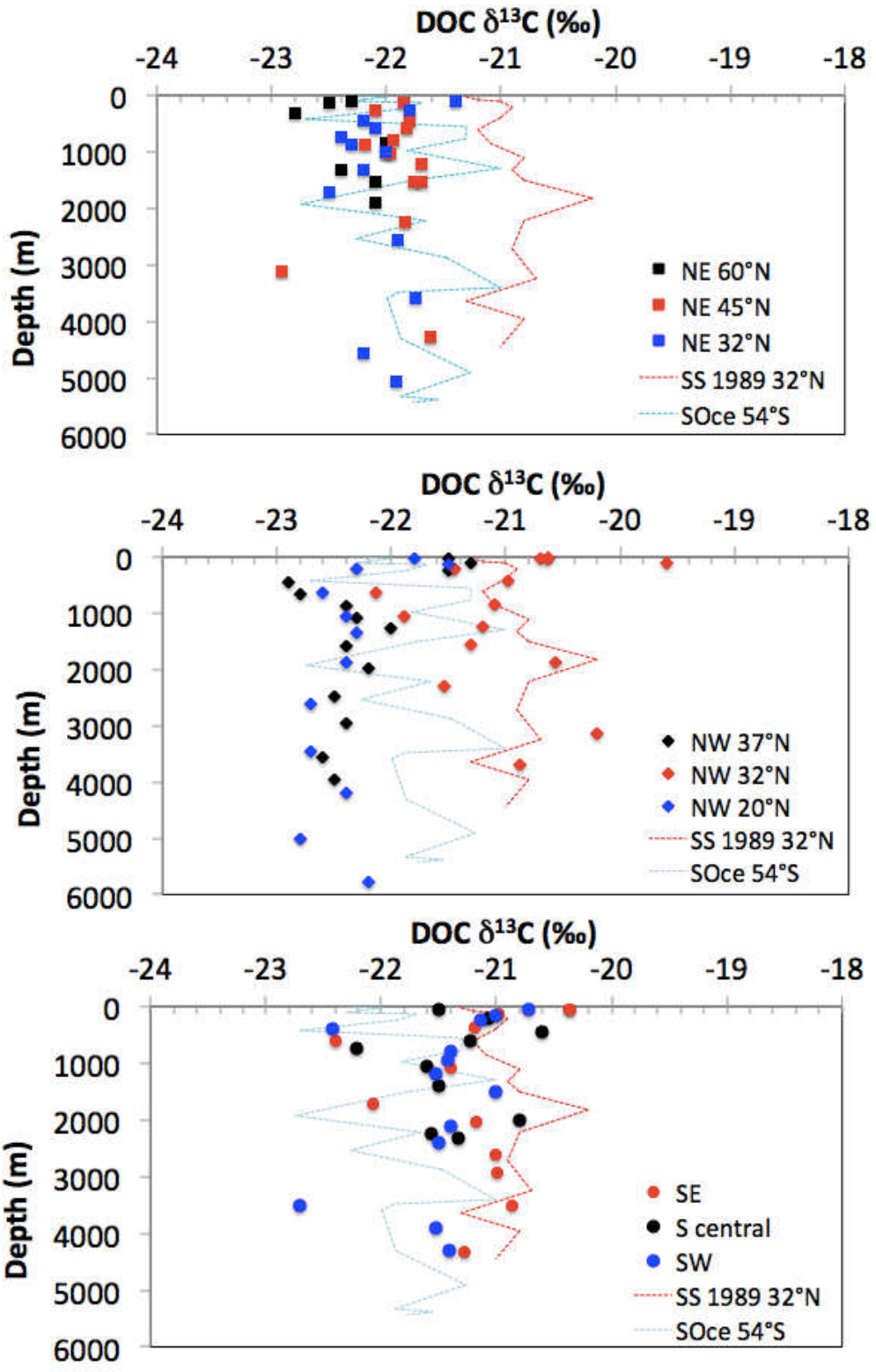

Figure S1. DOC $\delta^{13}C$ values in water samples collected from the a) NE Atlantic along 20°N (P16N), b) NW Atlantic along 65°N (A22 cruise), and c) South Atlantic along 32°S (A10 cruise). Values from the Sargasso Sea (SS) [*Druffel et al.*, 1992] and Southern Ocean (SOce) [*Druffel and Bauer*, 2000] cruises are shown for comparison.

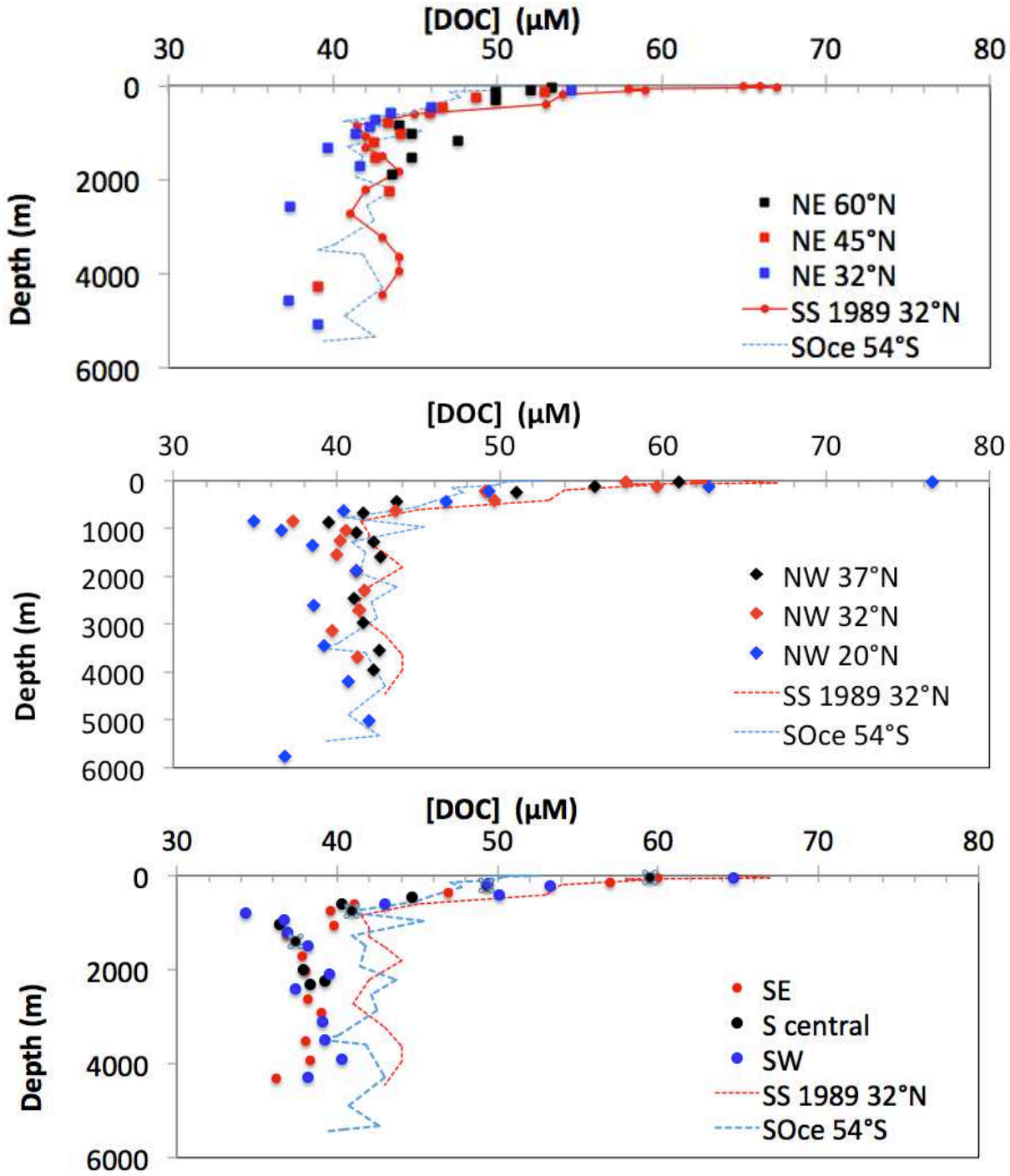

Figure S2. DOC concentrations in water samples collected from the a) NE Atlantic along 20°N (P16N), b) NW Atlantic along 65°N (A22 cruise), and c) South Atlantic along 32°S (A10 cruise). Values from the Sargasso Sea (SS) [*Druffel et al.*, 1992] and Southern Ocean (SOce) [*Druffel and Bauer*, 2000] cruises are shown for comparison.

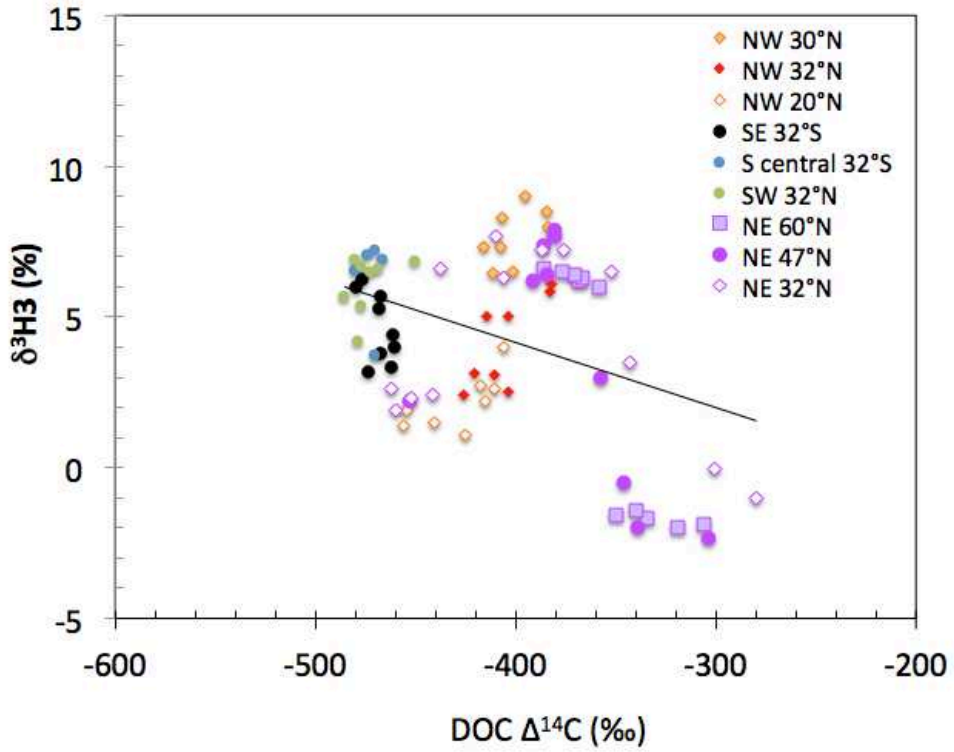

Figure S3. Ridge-flank systems have been shown to strip out oceanic DOC onto porous basalts [*Hawkes et al.*, 2015; *Lang et al.*, 2006] and deliver low $\Delta^{14}C$ DOC [*McCarthy et al.*, 2011] to the deep northeast Pacific. However, this effect may be more pronounced in the Pacific than in other oceans, because the spreading rates of ridges in the Pacific are the highest of all ocean ridge systems [*Lupton*, 1998]. Whereas ancient DOC from hydrothermal ridges and flanks may be important to the deep Pacific, this effect does not appear to be significant in the Atlantic DOC $\Delta^{14}C$ values (this work) versus $\delta^{3}He$ values obtained for samples from >1000m depth collected in 2003 or 1997 (along 65°W) from similar depths and locations as our samples from the A10, A22 and A16 cruises [*Jenkins*, 2007a; b; c]. Linear regression of all points shows an inverse correlation (r=0.38 p=0.0003 n=84). The values from the A22 (NW) and A16 (NE) cruises contain bomb ^{14}C, and the slope of this linear regression (0.022) is an order of magnitude smaller than that found for the South Pacific (0.297) [*Druffel and Griffin*, 2015] (see text for detail).

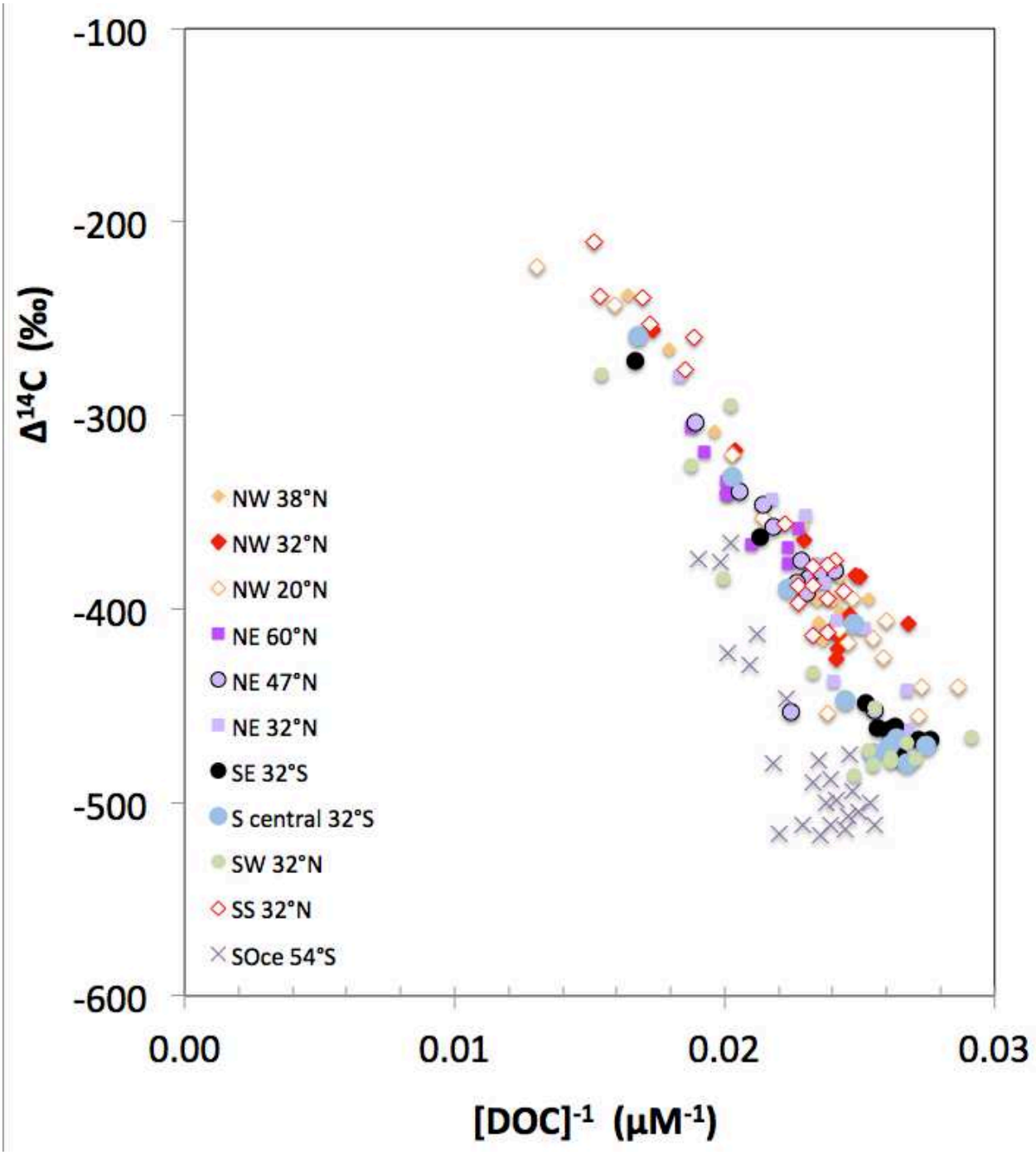

Figure S4. Keeling plot of measurements from the Atlantic Ocean as reported here, and the SOce and SS as reported elsewhere [*Druffel and Bauer*, 2000; *Druffel et al.*, 1992]. Slopes, y-intercepts and correlation coefficients are reported in Table S3.

Table S1. Sampling information for the stations occupied on the A10, A22 and A16N cruises in the Atlantic Ocean, and for the Sargasso Sea [*Druffel et al.*, 1992] and Southern Ocean [*Druffel and Bauer*, 2000] cruises.

Cruise/Stn.	Lat.	Long.	Date	Bottom depth (m)
A10 35	29° 59.444'S	01° 39.174'W	10/06/11	4650
A10 54	30° 00.002'S	13° 39.814'W	10/13/11	3012
A10 67	29° 59.988'S	23° 31.926'W	10/17/11	5025
A22 13	37° 51.068'N	68° 32.045'W	03/28/12	4460
A22 26	32° 38.846'N	64° 55.729'W	04/01/12	4047
A22 27	31° 54.456'N	65° 02.762'W	04/01/12	3878
A22 45	20° 01.730'N	65° 59.567'W	04/07/12	7417
A16N 10	60° 29.966'N	20° 0.017'W	08/05/13	2533
A16N 16	57° 30.010'N	19° 59.965'W	08/07/13	1164
A16N 36	47° 28.705'N	19° 59.654'W	08/11/13	4566
A16N 66	32° 30.110'N	21° 57.980'W	08/20/13	5212
SS	31° 50'N	63° 30' W	Jun-89	4450 ± 50
SOce	54° 00'S	176° 40'W	Dec-95	5332 ± 50

Table S2. Concentration, $\Delta^{14}C$ and ^{13}C measurements of bulk DOC in seawater samples collected on the A10, A16N and A22 cruises. These data, and other measurements of samples from the same niskin bottles, are available at http://cdiac.ornl.gov/ftp/oceans/CLIVAR/P06_2009/

Stn	UCID#	[DOC]	DOC Δ14C	DOC d13C	UCID#	DIC Δ14C
CTD dbars		μM	(‰)	(‰)		(‰)
A10 Stn 35						
49	16239	60.0	-272	-20.4		47
139	16243	56.9		-20.8		38
369	16214	46.9	-363	-21.2		43
609	17211	40.2	-409	-22.4		7
760	16211	39.6	-449			-26
1070	16249	39.8	-474	-21.4		-116
1245	16213	36.8	-468			-127
1719	16210	37.8	-476	-22.1		-131
2019	16206	38.0	-480	-21.2		-129
2620	16205	38.2	-467	-21.0		-123
2920	16203	39.0	-461	-21.0		-127
3520	16718	37.7	-461	-20.8		-123
3919	16204	38.3	-462			-128
4319	17212	35.4	-468	-21.5		-124
A10 Stn 54						
40	16713	60.6	-259	-21.9		47
40	16714	58.4				
210	16397	49.3	-332	-21.1		51
450	16424	44.7	-390	-20.6		40
600	16394	40.3	-408	-21.2		8
751	16700	40.9	-447	-22.2		-26
1050	16699	36.4	-471	-21.6		-88
1401	16697	35.3	-480	-21.3		-130
2000	16709	37.9	-467	-20.8		-126
2250	16396	39.2	-474	-21.6		-125
2310	16395	38.3	-471	-21.3		-125
A10 Stn 67						
40	16255	64.7	-279	-20.7		54
161	16404	56.6	-295	-21.5		54
225	16328	53.3	-326	-21.1		58
400	16393	50.1	-384	-22.4		51
600	16333	43.0	-433			13
801	16327	34.3	-466	-21.4		-38
951	16392	36.7	-477	-21.3		-70
1198	16720	36.9	-478	-21.5		-114
1500	16719	38.2	-477	-21.0		-129
2100	16388	39.5	-473	-21.4		
2400	16698	37.4	-469	-21.5		-117
3100	16326	39.1	-451			-114
3500	16405	39.2	-481	-22.7		-123
3900	16332	40.3	-486	-21.5		-138
4297	16324A	38.2	-479	-21.4		-147

Stn CTD dbars	UCID#	[DOC] μM	DOC Δ14C (‰)	DOC d13C (‰)	UCID#	DIC Δ14C (‰)
A22 Stn13						
22	17601	61.0	-237	-21.5		
118	17611	55.8	-266	-21.3		
239	17615	51.0	-308	-21.5		
439	17607	43.7	-357	-22.9		
671	17604	41.6	-395	-22.8		
871	17605	39.5	-395	-22.4		
1085	17610	41.2	-383	-22.3		
1276	17609	42.3	-384	-22.0		
1593	17612	42.7	-395	-22.4		
1969	17602		-407	-22.2		
2468	17606	41.1	-402	-22.5		
2966	17597	41.6	-411	-22.4		
3549	17598	42.6	-407	-22.6		
3955	17603	42.3	-416	-22.5		
A22 Stn26						
27	17206	62.2	-248	-21.0		58
1514	17217	40.9	-394	-22.1		-28
A22 Stn27						
37	17208	57.7	-256	-20.7		
111	17205	59.6	-258	-19.6		
218	17216	49.1	-318	-21.5		
419	17214	49.7	-340	-21.0		
639	17009	43.6	-364	-22.1		
842	17201	37.3	-407	-21.1		
1043	17202	40.6	-403	-21.9		
1247	16757	40.3	-382	-21.2		
1550	16756	40.0	-383	-21.3		
1884	16753	41.2	-414	-20.6		
2289	16752	41.7	-411	-21.5		
2697	16750	41.4	-426			
3143	16418		-404	-20.2		
3682	16748	41.3	-420	-20.9		
A22 Stn45						
35	17420A	76.5	-223	-21.8		
118	17418A	62.8	-243	-21.5		
216	17417A	49.3	-320	-22.3		
436	17415A	46.7	-353			
639	17413A	40.4	-395	-23.1		
839	17410A		-441			
1043	17409A	36.6	-441	-22.4		
1346	17407A	38.5	-406	-22.3		
1885	17406A	41.2	-411	-22.4		
2613	17293A	38.6	-425	-22.7		
3446	17294A	39.2	-415	-22.7		
4199	17292A	40.7	-418	-22.4		
5019	17291A	42.0	-454	-22.8		
5767	17422	36.8	-456	-22.2		

Stn CTD dbars	UCID#	[DOC] μM	DOC Δ14C (‰)	DOC d13C (‰)	UCID#	DIC Δ14C (‰)
A16N Stn10						
44	17968	53.3	-306			
94	17966	52.0	-319	-22.3		
141	17974	49.9	-334	-22.5		
306	17969A	49.9	-341	-22.8		
847	17967	44.0	-358	-22.0		
1012	17970	44.8	-368	-22.0		
1164	17982	47.6	-367			
1313	17965		-370	-22.4		
1538	17975	44.8	-377	-22.1		
1901	17976	43.6	-386	-22.1		
A16N Stn16						
69	18196	53.8	-302	-22.0		
A16N Stn36						
37						
125	18276	52.9	-303	-21.9		
262	18292	48.7	-339	-22.1		
450	18275	46.7	-346	-21.8		
575	18195	45.9	-357	-21.8		
783	18283	43.3	-384	-21.9		
875	18295	41.5	-418	-22.2		
1025	18280	44.1	-386	-22.0		
1200	18291	42.5	-380	-21.7		
1525	18294	42.6	-378	-21.8		
2250	18198	43.4	-391	-21.8		
3100	18695	44.5	-453	-22.9		
4275	18286	39.1	-453	-21.6		
A16N Stn66						
116	18175	54.5	-280	-21.4		
263	17960		-301	-21.8		
451	18191	46.0	-343	-22.2		
575	18166	43.5	-352	-22.1		
725	18182	42.6	-376	-22.4		
875	18167	42.2	-387	-22.3		
1014	18174	41.4	-406	-22.0		
1325	18181	39.7	-410	-22.2		
1725	18176	41.6	-437	-22.5		
2569	17961	37.4	-442	-21.9		
3576	18184		-460	-21.8		
4576	18179	37.3	-462	-22.2		
5075	18185	39.1	-452	-21.9		

Table S3. DOC Keeling plot slopes, intercepts and correlation coefficients determined from Model II linear regressions. Values from the South Pacific (P06 in 2010) [*Druffel and Griffin*, 2015], NCP (1987), Sargasso Sea (1989) [*Druffel et al.*, 1992], and SOce (1995) [*Druffel and Bauer*, 2000] are included for comparison. Available surface DIC $\Delta^{14}C$ values are included for comparison with the intercept values.

Cruise/Stn.	Slope	Slope error	Intercept	Intercept error	r^2, n	Surface DIC $\Delta^{14}C$ [a]
A10 35	-19577	1496	50	37	0.98, 13	47 ± 4
A10 54	-22265	1758	117	41	0.94, 10	47 ± 4
A10 67	-19247	2583	35	56	0.80, 15	54 ± 4
A22 13	-21184	1807	111	40	0.93, 13	
A22 27	-18901	2108	62	45	0.87, 14	58 ± 4
A22 45	-16843	1532	10	34	0.91. 14	
A16N 10	-22919	2550	132	51	0.90, 9	
A16N 36	-20921	4750	89	102	0.9, 12	
A16N 66	-22919	2581	152	59	0.90, 11	
P06 130	-25104	2447	188	61	0.94, 9	78 ± 3
P06 190	-23138	1175	145	30	0.97, 14	74 ± 3
P06 218	-21983	952	110	24	0.98, 15	61 ± 3
P06 228	-21656	1430	84	37	0.97, 9	40 ± 3
P06 248	-21935	1629	112	39	0.97, 7	25 ± 3
NCP	-24136	1181	159	29	0.97, 38	131 ± 13
SS	-21962	1427	126	29	0.94, 17	114 ± 10
SOce	-25639	3358	116	66	0.73, 24	16 ± 8

[a] For all Atlantic profiles reported here, the single sample between 0–100m was used; SOce mean 3–50m depth; SS mean 3–100m; NCP mean 3–100m.

References

Druffel, E., and J. Bauer (2000), Radiocarbon distributions in Southern Ocean dissolved and particulate organic carbon, *Geophysical Research Letters*, *27*, 1495-1498.
Druffel, E., and S. Griffin (2015), Radiocarbon in dissolved organic carbon of the South Pacific Ocean, *Geophys. Res. Lett.*, *42*, 4096-4101.
Druffel, E., P. Williams, J. Bauer, and J. Ertel (1992), Cycling of dissolved and particulate organic matter in the open ocean, *Journal of Geophysical Research*, *97*, 15639-15659.
Hawkes, J., et al. (2015), E-fficient removal of recalcitrant deep-ocean dissolved organic matter during hydrothermal circulation, *Nature Geoscience*, *8*, 856-861.
Jenkins, W. (2007a), Tritium and helium-3 data from A10 cruise in 2003, edited by CChdo.ucsd.edu/cruise, CCHDO.
Jenkins, W. (2007b), Tritium and helium-3 data from A22 cruise in 2003, edited by CChdo.ucsd.edu/cruise, CCHDO.
Jenkins, W. (2007c), Tritium and helium-3 data from A16 cruise in 2003, edited by CChdo.ucsd.edu/cruise, CCHDO.
Lang, S., D. Butterfield, M. Lilley, H. Johnson, and J. Hedges (2006), Dissolved organic carbon in ridge-axis and ridge-flank hydrothermal systems, *Geochimica et Cosmochimica Acta*, *70*, 3830-3842.
Lupton, J. (1998), Hydrothermal helium plumes in the Pacific Ocean, *J Geophysical Research*, *103*(C8), 15853-15868.
McCarthy, M., S. Beaupré, B. Walker, I. Voparil, T. Guilderson, and E. Druffel (2011), Chemosynthetic origin of 14C-depleted dissolved organic matter in a ridge-flank hydrothermal system, *Nature Geoscience*, *4*, 32-36.